Comparative Analysis of Guided Modal Properties of Double-Positive and Double-Negative Metamaterial Slab Waveguides

Ki Young KIM

Dept. of Physics, National Cheng Kung University, 1 University Road, Tainan 70101, Taiwan, Republic of China

kykim1994@gmail.com

Abstract. *The guided modal properties of double-positive and double-negative metamaterial slab waveguides are numerically analyzed and compared when varying the dielectric and magnetic constants. As the cutoff frequencies of both slab waveguides remained unchanged when the absolute value of the refractive index was kept invariant, this enabled an effective comparison of the respective guided modes. Thus, the guided mode dispersion characteristics of the double-positive and double-negative slab waveguides were analyzed and compared, including several higher order modes. As a result, this comparative analysis provides greater physical insights and a better understanding of the guided modal characteristics of double-negative metamaterial slab waveguides.*

Keywords

Double-negative index, double-positive index, guided mode dispersions, metamaterial slab waveguide, surface polariton, surface wave.

1. Introduction

Based on Pendry's ideas of practical realizations for artificial negative permittivity [1], [2] and permeability [3], Veselago's theoretical predictions for simultaneously negative material indexes [4] were experimentally verified by Smith et al. [5], [6]. Since then, a lot of theoretical and experimental work has been undertaken in relation to both the novel physics of these unusual materials and their practical and unique applications to microwave and optical devices [7-9]. Among such applications, planar guiding structures with double-negative (DNG) metamaterial inclusions have attracted much interest as regards their fundamental modal properties and different applications [10-44], as double-positive (DPS) dielectric slab waveguides are commonly used in microwave and optics regimes. The modal properties of grounded DNG slabs [10-19], DNG slabs with symmetric [20-28] and asymmetric [28-35] dielectric claddings, DNG multilayers [36-38], air- or dielectric-filled gaps embedded in DNG materials [39-41], and dielectric slabs with a DNG cover or substrate [42-44] have already been investigated and resulted in several important findings, including a sign-varying power flux [13, 21], the absence of a fundamental mode [16, 17, 33], a zero or negative group velocity [18, 25, 34], the coexistence of eigenmodes [23, 31, 33, 34, 41], and an evanescent field enhancement [28]. Thus, numerous potential applications have been suggested using these geometries with DNG material inclusions, such as a backward wave generator [13], compact resonator and phase shifters [14], bandpass filter [14, 23], contradirectional coupler [24], optical imager [35], energy-transfer enhancer [35], high capacity storage [37], anti- and high-reflection coatings [38], nano-optical waveguide [41], and ultrasensitive optical sensor [41]. Nonetheless, relatively little attention has been focused on a comparative analysis of DNG slab waveguides and DPS slab waveguides, despite the potential importance in terms of understanding DNG slab waveguides in more detail.

Accordingly, this study conducted a comprehensive comparative analysis of the guided modal properties of DNG and DPS slab waveguides in order to provide greater physical insights and a better understanding of the physical phenomena related to DNG slab waveguides. The guided modal properties of slab waveguides with several simultaneously positive and negative material constant sets with identical absolute values for the refractive index are investigated for both DPS and DNG slab waveguides to facilitate a comparative analysis of the guided modal dispersion characteristics. In addition, the guided modal properties of DNG slab waveguides are also briefly compared with those of other relevant geometrical and material configurations, such as a grounded DNG slab, DNG gap, and plasmonic/plasma slab.

2. Characteristic Equations of Ordinary Surface and Surface Polariton Modes

Fig. 1 shows a symmetric DPS or DNG slab waveguide structure with a height of 2h, placed in a free space

region, along with four possible distinctive field configurations in the transverse x-direction. The propagation of the electromagnetic waves is in the $+z$ direction. The dielectric and magnetic constants (relative permittivity and relative permeability) are denoted by ε_{ri} and μ_{ri} (i = 1, 2), respectively, while subscripts 1 and 2 represent the slab ($x < |h|$) and surrounding free space ($x > |h|$) regions, respectively. Various dielectric and magnetic constants were chosen for the slab, i.e. ε_{r1} and μ_{r1}, yet $\varepsilon_{r2} = \mu_{r2} = 1.0$ was assumed for the free space region.

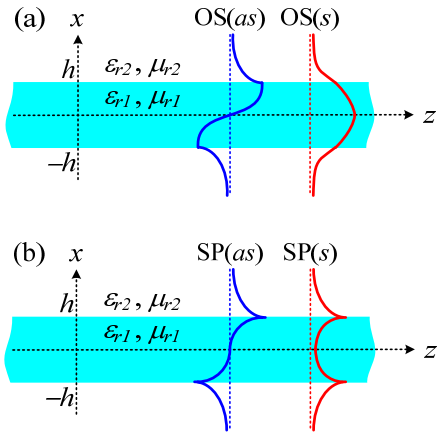

Fig. 1. Schematic illustration of symmetric slab waveguide and sketches of field profiles for (a) surface polariton (SP) and (b) ordinary surface (OS) modes. The asymmetric and symmetric modes are denoted by "*as*" and "*s*", respectively.

Following the standard steps in boundary-value problems, i.e. enforcing continuation of the fields at interfaces between the slab and free space regions, the characteristic equations can be derived. The characteristic equations of the TM_m mode for asymmetric (m = 0,2,4,…) and symmetric (m = 1,3,5,…) modes, as shown in Fig. 1(a), can be obtained respectively as follows:

$$k_1\varepsilon_{r2}\tan(k_1h) - k_2\varepsilon_{r1} = 0\,, \tag{1}$$

$$k_1\varepsilon_{r2}\cot(k_1h) + k_2\varepsilon_{r1} = 0 \tag{2}$$

where k_1 and k_2 are the transverse propagation constants in the slab and free space regions, and given by $k_1 = k_0(\mu_{r1}\varepsilon_{r1} - \bar{\beta}^2)^{1/2}$ and $k_2 = k_0(\bar{\beta}^2 - \mu_{r2}\varepsilon_{r2})^{1/2}$, respectively, in which case $\bar{\beta}\,(=\beta/k_0)$ is the normalized propagation constant and k_0 is the free space wave number. Here, the allowed guided mode region for the normalized propagation constant is $\mu_{r2}\varepsilon_{r2} < \bar{\beta} < \mu_{r1}\varepsilon_{r1}$, which is the same as that of the surface waves in a conventional dielectric slab waveguide [45]. As such, this mode is called the ordinary surface (OS) mode in this study, which can be supported in both DPS and DNG slab waveguides.

However, under certain conditions in the case of DNG slab waveguides, the normalized propagation constant can transcend the higher limit of the OS mode due to the negative indexes, i.e. $\bar{\beta} > (\mu_{r1}\varepsilon_{r1})^{1/2}$. In this situation, the transverse propagation constant in the slab region is given by $k_1 = k_0(\bar{\beta}^2 - \mu_{r1}\varepsilon_{r1})^{1/2}$, the same as k_2. Since the field configurations of this mode are exponentially decaying in both transverse directions from the interface, as shown in Fig. 1(b), which is similar to the surface plasmon polariton at a metal/dielectric interface [46], this mode is called the surface polariton (SP) mode in this study and only a monomodal property is expected. Consequently, from the boundary-value problems for this condition, the characteristic equations of the asymmetric ($m = 0,2,4,\cdots$) and symmetric ($m = 1,3,5,\cdots$) TM_m modes for the SP modes can also be obtained respectively as follows:

$$k_1\varepsilon_{r2}\tanh(k_1h) + k_2\varepsilon_{r1} = 0\,, \tag{3}$$

$$k_1\varepsilon_{r2}\coth(k_1h) + k_2\varepsilon_{r1} = 0\,. \tag{4}$$

The resultant characteristic equations (3) and (4) for the SP modes of DNG slab waveguides are the same as those for single-negative (SNG) slab waveguides that include plasma or plasmonic slabs [47-49].

It should be noted that the characteristic equations for the TE modes can be easily obtained by interchanging the dielectric and magnetic constants with each other based on the duality principle, and the modal properties of the TM and TE modes are also identical if both material constants are thought to be interchangeable, which has already been confirmed in part in the case of grounded DNG slab waveguides [10]. Thus, only the TM mode characteristics will be investigated in this study.

3. Numerical Results and Discussion

The guided modal properties of slab waveguides can be analyzed in terms of their dispersion curves, i.e. normalized propagation constant versus normalized frequency (k_0h), which are solutions of the characteristic equations (1) to (4) outlined in the previous section. First, the modal behavior of DPS slab waveguides is investigated with several combinations of simultaneously positive dielectric and magnetic constants. The DPS and DNG materials considered here were assumed to be isotropic and homogeneous magneto-dielectric materials [50] with potentially non-unity magnetic constants. Fig. 2 shows the dispersion curves of the asymmetric and symmetric TM_m modes for five different DPS material combination sets, i.e. { ε_{r1} , μ_{r1} }={+0.5, +8.0}, {+1.0, +4.0}, {+2.0, +2.0}, {+4.0, +1.0}, and {+8.0, +0.5}, which were chosen to investigate how dissimilar DPS material sets with the same positive refractive index, i.e. $n_1 = (\mu_{r1}\varepsilon_{r1})^{1/2} = +2.0$, would affect the modal properties of the waveguide. Note the set of $\varepsilon_{r1} = +4.0$ and μ_{r1}=+1.0 corresponded to conventional dielectric materials. The normalized cutoff frequencies, where the normalized propagation constant is the same as that of the embedding free space, i.e. $\bar{\beta}$=1.0 , were not changed for any of the DPS material constant combinations

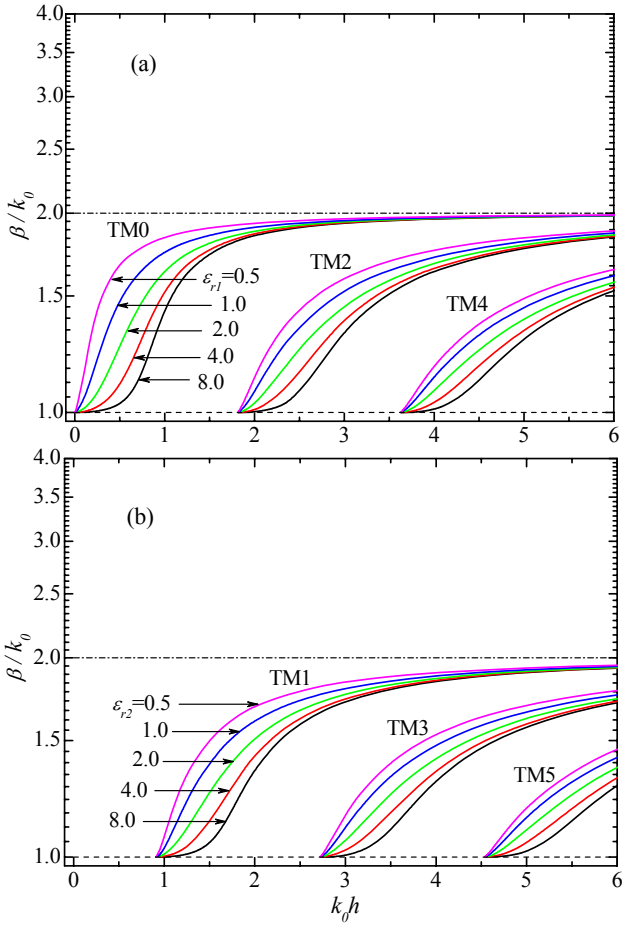

Fig. 2. Guided dispersion characteristics of double-positive slab waveguides. (a) Asymmetric and (b) symmetric modes.

TM0	TM1	TM2	TM3	TM4
0	0.907	1.814	2.721	3.628

Tab. 1. Normalized cutoff frequency of TM_m mode.

and are listed in Tab. 1. There was no normalized cutoff frequency for the TM_0 mode and its normalized propagation constant approached unity as the normalized frequency was decreased, which is already well known for conventional dielectric slab waveguides. In the case of conventional dielectric slab waveguides with different dielectric constants yet a fixed magnetic constant of unity, the normalized propagation constant increases with a higher dielectric constant for the slab, and exhibits a higher field concentration inside the slab region. However, for the DPS metamaterial slab waveguides in this study, it is interesting to note that the normalized propagation constant had a lower value with higher dielectric constants (yet lower magnetic constants), and exhibited a less confined field inside the slab region. As expected, the guided modes remained within the region of $\mu_{r2}\varepsilon_{r2} < \bar{\beta} < \mu_{r1}\varepsilon_{r1}$ for both the asymmetric and symmetric modes and the dispersion curves followed a well-behaved tendency with respect to the material constant variations, despite the use of unconventional material constants of less than unity, such as $\varepsilon_{r1} = +0.5$ or $\mu_{r1}=+0.5$.

Next, the guided modal properties of the DNG slab waveguides were considered with several negative material sets. Fig. 3 shows the guided dispersion characteristics of the DNG slab waveguides with several sets of simultaneously negative dielectric and magnetic constants of $\{\varepsilon_{r1}, \mu_{r1}\}$={–0.5, –8.0}, {–0.8, –5.0}, {–1.0, –4.0}, {–2.0, –2.0}, {–4.0, –1.0}, and {–8.0, –0.5}. Similar to the previous DPS metamaterial cases, each material set was chosen to generate an identical negative refractive index of $n_1 = -(\mu_{r1}\varepsilon_{r1})^{1/2} = -2.0$. In the case of the grounded DPS and DNG slab waveguides, all the symmetric TM_m modes were suppressed by the electrical symmetry at $x = 0$ (in Fig. 1), leaving only asymmetric TM_m modes [10, 14], which is different from the present structure. As shown in Fig. 3(a), the principal modes of the asymmetric and symmetric TM_m modes, i.e. the TM_0 and TM_1 modes, were quite different from those in the DPS slab waveguides shown in Figs. 2 (a) and (b). In the case of $|\varepsilon_{r1}| \geq 1.0$, all the TM_0 modes were suppressed, as predicted by Baccarelli et al. [17]. Meanwhile, all the TM_1 modes existed in the form of backward waves with negative slopes in the dispersion curves for every material combination set considered here. The normalized cutoff frequencies of the TM_1 mode for all the material constant sets considered in Fig. 3(a) were identical at $k_0h = 0.907$, which was the same as that for the DPS slab waveguides shown in Tab. 1. This indicates that the normalized cutoff frequency of the slab waveguide remained invariant, even for simultaneously negative dielectric and magnetic constants, when the absolute value of the refractive index was kept the same. This was also true for the higher order modes of the DNG slab waveguides, as shown in Figs. 3(b) and (c). As the normalized frequency decreased, the normalized propagation constants of the TM_1 mode increased to the SP mode region, corresponding to the symmetric field configuration in Fig. 1(b), indicating that the solutions of the characteristic equations (2) and (4) were seamlessly continued over the OS and SP mode regions at $\bar{\beta} = 2.0$ to complete the guided modal properties of the TM_1 mode.

When also considering the cases of $|\varepsilon_{r1}| < 1.0$, i.e., $\varepsilon_{r1} = -0.8$ and $\mu_{r1} = -5.0$ ["A" in Fig. 3(a)]; $\varepsilon_{r1} = -0.5$ and $\mu_{r1} = -8.0$ ["B" in Fig. 3(a)], the TM_0 modes that were suppressed in the case of $|\varepsilon_{r1}| \geq 1.0$ were found to exist in the form of a backward wave in a lower normalized frequency region. However, while the TM_0 mode in this case had no cutoff, making it similar to the TM_0 mode in the DPS slab, the normalized propagation constants approached to infinity as the normalized frequency decreased, whereas those of the TM_0 modes for the DPS slab waveguides approached to unity. As such, a higher electromagnetic field concentration inside the slab region can not be expected based on reducing the height of the DPS slab waveguide. In contrast, the principal modes of the DNG slab waveguide were tightly confined in the form

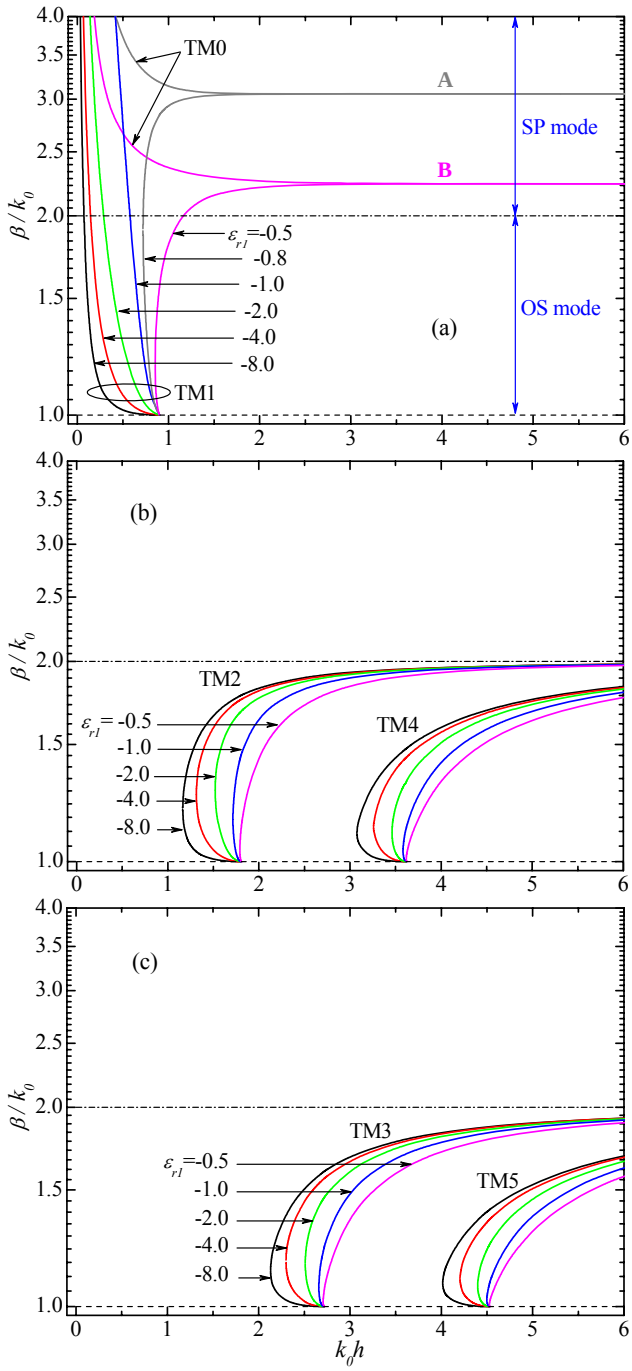

Fig. 3. Guided dispersion characteristics of double-negative slab waveguides. (a) Principal modes of asymmetric and symmetric modes, (b) higher order modes of asymmetric modes, and (c) higher order modes of symmetric modes.

of backward waves inside the slab region due to the very slow phase velocity (k_0/β). Thus, reducing the height of the DNG slab waveguide to a subwavelength scale can produce a higher field concentration inside the slab region for use in compact transmission line applications. As the normalized frequency increased, the normalized propagation constants of the TM_0 mode for the cases of "A" and "B" asymptotically approached the values of $\beta/k_0 = 3.055$ and $\beta/k_0 = 2.236$, respectively, which only belonged to the SP mode region. Therefore, no continuation of the normalized propagation constants over the OS and SP modes was observed, as distinct from the previous case of the TM_1 mode. In the case of the plasmonic slab waveguides, the TM_0 and TM_1 modes both existed as SP modes, which is the only propagation mechanic for this waveguide. Meanwhile, the TM_0 mode of the DNG slab waveguides resembled that of the plasmonic slab [48], whereas the TM_1 mode of the DNG slab also had solutions in the OS mode region, as mentioned, due to the DNG index, which differed from the case of the plasmonic slab. Furthermore, the TM_1 modes for $|\varepsilon_{r1}| < 1.0$ exhibited forward waves with a positive slope in the dispersion curves, while the normalized propagation constant asymptotically approached to $\beta/k_0 = 3.055$ and $\beta/k_0 = 2.236$ for cases "A" and "B", respectively. Eventually, the TM_0 and TM_1 modes exhibited common guided modal properties for $|\varepsilon_{r1}| < 1.0$ with a higher normalized frequency regime, despite their different field profiles, as shown in Fig. 1(b). This phenomenon only occurred in the SP mode region at higher normalized frequencies, i.e. with a higher physical frequency or thicker slab. At this higher normalized frequency, the SP modes at both interfaces, i.e. at $x = \pm h$, were essentially decoupled with each other inside the slab region, giving the appearance of a single interface between the free space and the DNG half space. In other words, the SP modes at $x = \pm h$ appeared to be independent. The normalized propagation constant of the single interface for the TM mode with a non-unity negative dielectric and magnetic constants in region 1 was derived as follows:

$$\beta/k_0 = \sqrt{\frac{\varepsilon_{r1}\varepsilon_{r2}\left(\varepsilon_{r1}\mu_{r2} - \mu_{r1}\varepsilon_{r2}\right)}{\varepsilon_{r1}^2 - \varepsilon_{r2}^2}}. \qquad (5)$$

If the surface plasmon polaritons at a single metal/dielectric interface is considered with unity magnetic constants in each region, equation (5) can be reduced to $\beta/k_0 = [\varepsilon_{r1}\varepsilon_{r2}/(\varepsilon_{r1}+\varepsilon_{r2})]^{1/2}$, which is well known [46], and the TE mode version of equation (5) can also be derived in a similar way [49]. Thus, for the cases of "A" ($\varepsilon_{r1} = -0.8$ and $\mu_{r1} = -5.0$) and "B" ($\varepsilon_{r1} = -0.5$ and $\mu_{r1} = -8.0$) in Fig. 3(a), the normalized propagation constants from equation (5) were $\beta/k_0 = 3.055$ and $\beta/k_0 = 2.236$, respectively, which were identical to the normalized propagation constants obtained from the characteristic equations (3) and (4) for a higher normalized frequency regime. Thus, it was confirmed that this phenomenon was not just a coincidence, but resulted from the surface polaritons at a single interface. This was also found in cases of DNG gap [41] and SNG slab [48, 49] waveguides. However, this phenomenon is hardly seen in the OS mode region, as the electromagnetic fields inside the slab region are oscillatory rather than evanescent in the transverse direction and more or less coupled with each other.

Figs. 3(b) and (c) show the dispersion curves of the higher order asymmetric and symmetric TM_m modes for the DNG slab waveguides, respectively, when using the same absolute values for the material sets as those considered in Figs. 2(a) and (b). Forward and backward waves always coexisted and their normalized cutoff frequencies did not change with the various material constant combinations, even in the case of negative material constants, as mentioned previously. The backward wave propagation region, extending from the bifurcation point (meeting point of the forward and backward waves) to the normalized cutoff frequency, became wider when increasing the absolute value of the dielectric constants. As the dielectric constants were increased, the normalized propagation constants of the backward waves also increased, as with the DPS slab waveguides, as shown in Fig. 2, however, the forward waves of the DNG slab waveguides had lower normalized propagation constants, which was contrary to the case of the DPS slab waveguides. Thus, the forward waves of the DPS and DNG slab waveguides would be expected to be closer with higher absolute values for both dielectric constants.

Fig. 4(a) shows the guided modal properties of the DPS and DNG slab waveguides for $\varepsilon_{r1} = \pm 8.0$ and $\mu_{r1} = \pm 0.5$, as an exemplary case of higher absolute values for both dielectric constants of the DPS and DNG materials. As mentioned previously, the TM_0 mode of the DNG slab was suppressed and the normalized cutoff frequencies were the same for both cases. It is interesting to note that with a higher normalized frequency far above from the normalized cutoff frequency, the normalized propagation constant of the forward TM_2 (TM_3) mode for the DNG slab approached that of the TM_0 (TM_1) mode for the DPS slab, and the other higher order modes also followed this tendency. This phenomenon was probably due to the absence of the principal forward TM modes for the DNG slab in the OS mode region. In other words, since the forward TM_2 mode of the DNG slab was actually the first asymmetric forward wave in the OS mode, it tended to behave like the first asymmetric mode of the DPS slab waveguide. Likewise, since the forward TM_3 mode of the DNG slab played the role of the first forward symmetric mode in the OS mode region, it followed the modal behavior of the TM_1 mode as the first symmetric mode of the DPS slab waveguide. Fig. 4(b) shows the guided dispersion characteristics of the DPS and DNG slab waveguides for $\varepsilon_{r1} = \pm 0.8$ and $\mu_{r1} = \pm 5.0$, as an exemplary case of low absolute values for the dielectric constants to compare with the previous case in Fig. 4(a). As in the previous case, the forward TM_2 (TM_3) mode of the DNG slab waveguide approached the TM_0 (TM_1) mode of the DPS slab waveguide with a higher normalized frequency in the OS mode region, however, it was not as clear as the case shown in Fig. 4(a), probably due to the existence of the forward TM_1 mode in the DNG slab waveguide.

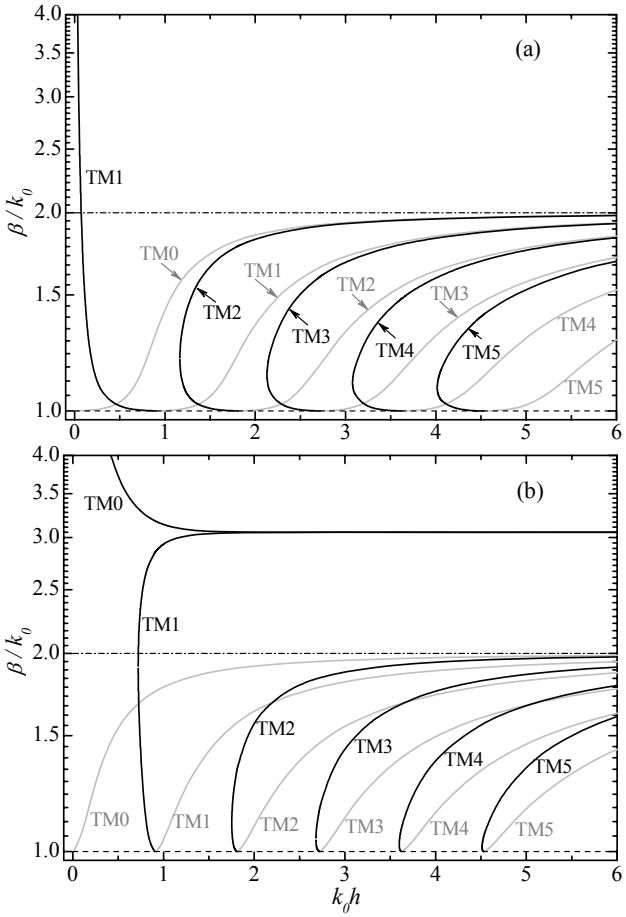

Fig. 4. Guided dispersion characteristics of double-positive and double-negative slab waveguides for (a) $\varepsilon_{r1} = \pm 8.0$ and $\mu_{r1} = \pm 0.5$, and (b) $\varepsilon_{r1} = \pm 0.8$ and $\mu_{r1} = \pm 5.0$. The black and grey lines denote the DNG and DPS slab waveguides, respectively.

4. Conclusion

The guided modal characteristics of DPS and DNG slab waveguides were comparatively investigated as regards the OS and SP modes using several combinations of dielectric and magnetic constants with identical absolute values for the refractive index. For both the DPS and DNG slab waveguides, the normalized cutoff frequencies remained invariant for all the selected material constants, even when inversing the material signs, thereby enabling an effective comparison of the guided modal properties. As a result, the extensive comparative analysis conducted in this study provides greater physical insights and a better understanding of the guided modal dispersion properties of DNG metamaterial slab waveguides. Although the comparative guided modal characteristics were only analyzed for a basic symmetric slab waveguide structure, the results are also valid for asymmetric slab waveguides.

References

[1] PENDRY, J. B., HOLDEN, A. J., STEWART, W. J., YOUNGS, I. Extremely low frequency plasmons in metallic microstructures. *Physical Review Letters,* 1996, vol. 76, no. 25, p. 4773 - 4776.

[2] PENDRY, J. B., HOLDEN, A. J., ROBBINS, D. J., STEWART, W. J. Low frequency plasmons in thin wire structures. *Journal of Physics: Condensed Matters,* 1998, vol. 10, no. 22, p. 4785 - 2084.

[3] PENDRY, J. B., HOLDEN, A. J., ROBBINS, D. J., STEWART, W. J. Magnetism from conductors and enhanced nonlinear phenomena. *IEEE Transactions on Microwave Theory and Techniques,* 1999, vol. 47, no. 11, p. 2075 - 2084.

[4] VESELAGO, V. G. The electrodynamics of substances with simultaneously negative values of ε and μ. *Soviet Physics Uspekhi*, 1968, vol. 10, no. 4, pp. 509 - 514.

[5] SMITH, D. R., PADILLA, W. J., VIER, D. C., NEMAT-NASSER, S. C., SCHULTZ, S. Composite medium with simultaneously negative permeability and permittivity. *Physical Review Letters*, 2000, vol. 84, no. 18, pp. 4184 - 4187.

[6] SHLBY, R. SMITH, D. R., SCHULTZ, S. Experimental verification of a negative index of refraction. *Science*, 2001, vol. 292, no. 5514, p. 77 - 79.

[7] ENGHETA, N., ZIOLKOWSKI, R. W. A positive future for double-negative metamaterials. *IEEE Transactions on Microwave Theory and Techniques*, 2005, vol. 53, no. 4, p. 1535 - 1556.

[8] ENGHETA, N. ZIOLKOWSKI, R. W. Eds. *Metamaterials: Physics and Engineering Explorations*. John Wiley & Sons, Inc., 2006.

[9] ELEFTHERIADES, G. V., BALMAIN, K. G. Eds. *Negative-Refraction Metamaterias: Fundamental Principles and Applications*. John Wiley & Sons, Inc., 2005.

[10] KIM, K. Y., CHO, Y. K., TAE, H.–S., LEE, J.–H. Guided mode propagation of grounded double-positive and double-negative metamaterial slabs with arbitrary material indexes. *Journal of the Korean Physical Society*, 2006, vol. 49, no. 2, p. 577 - 584.

[11] LOVAT, G., BURGHIGNOLI, P., YAKOVLEV, A. B., HANSON, G. W. Modal interactions in resonant metamaterial slabs with losses. *Metamaterials*, 2008, vol. 2, no. 4, p. 198 - 205.

[12] MAHMOUD, S. F., VIITANEN, A. J. Surface wave character on a slab of metamaterial with negative permittivity and permeability. *Progress in Electromagnetics Research*, 2005, vol. 51, p. 127 to 137.

[13] SHELLENG, J., MONZON, C., LOSCHIALPO, P. F., FORESTER, D. W., MEDGYESI-MITSCHANG, L. N. Characteristics of waves guided by a grounded "left-handed" material slab of finite extent. *Physical Review E*, 2004, vol. 70, no. 6, 066606.

[14] SUWAILAM, M. M. B., CHEN, Z. Z. Surface waves on a grounded double-negative (DNG) slab waveguide. *Microwave and Optical Technology Letters*, 2005, vol. 44, no. 6, p. 494 - 498.

[15] DONG, H., WU, T. X. Analysis of discontinuities in double-negative (DNG) slab waveguides. *Microwave and Optical Technology Letters*, 2003, vol. 39, no. 6, p. 483 - 488.

[16] BACCARELLI, P., BURGHIGNOLI, P., FREZZA, F., GALLI, A., LAMPARIELLO, P., LOVAT, G., PAULOTTO, S. Fundamental modal properties of surface waves on metamaterial grounded slabs. *IEEE Transactions on Microwave Theory and Techniques*, 2005, vol. 53, no. 4, p. 1431 - 1442.

[17] BACCARELLI, P., BURGHIGNOLI, P., LOVAT, G., PAULOTTO, S. Surface-wave suppression in a double-negative metamaterial grounded slab. *IEEE Antennas and Wireless Propagation Letters*, 2003, vol. 2, p. 269 - 272.

[18] SHU, W., SONG, J. M. Complete mode spectrum of a grounded dielectric slab with double negative metamaterials. *Progress in Electromagnetics Research*, 2006, vol. 65, p. 103 - 123.

[19] LI, C., SUI, Q., LI, F. Complex guided wave solutions of grounded dielectric slab made of metamaterials. *Progress in Electromagnetics Research*, 2005, vol. 51, p. 187 - 195.

[20] RUPPIN, R. Surface polaritons of a left-handed material slab. *Journal of Physics: Condensed Matters*, 2001, vol. 13, no. 9, p. 1811 - 1819.

[21] SHADRIVOV, I. V., SUKHORUKOV, A. A., KIVSHAR, Y. S. Guided modes in negative-refractive-index waveguides. *Physical Review E*, 2003, vol. 67, no. 5, 057602.

[22] WU, B.–I., GRZEGORCZYK, T. M., ZHANG, Y., KONG, J. A. Guided modes with imaginary transverse wave number in a slab waveguide with negative permittivity and permeability. *Journal of Applied Physics*, 2003, vol. 93, no. 11, p. 9386 - 9388.

[23] CORY, H., BARGER, A. Surface-wave propagation along a metamaterial slab. *Microwave and Optical Technology Letters*, 2003, vol. 38, no. 5, p. 392 - 395.

[24] ALÙ, A., ENGHETA, N. An overview of salient properties of guided-wave structures with double-negative and single-negative metamaterials. In *Negative Refraction Metamaterials: Fundamental Properties and Applications*, ELECFTHERIADES, G. V., BALMAIN, K. G. Eds., John Wiley & Sons, Inc., 2005.

[25] VUKOVIĆ, S. M., ALEKSIĆ, N. B., TIMOTIJEVIĆ, D. V. Guided modes in left-handed waveguides. *Optics Communications*, 2008, vol. 281, no. 6, p. 1500 - 1509.

[26] CHIU, K. P., TSAI, D. P. Characteristics of plasmonic resonance in a sandwiched metamaterial nano film. *Optical and Quantum Electronics*, 2006, vol. 38, no. 12-14, p. 1011 - 1017.

[27] REZA, A. *The Optical Properties of Metamaterial Waveguide Structures*. M. S. Thesis, Queen's University, 2008.

[28] CHIU, K. P., KAO, T. S., TSAI, D. P. Evanescent field enhancement due to plasmonic resonances of a metamaterial slab. *Journal of Microscopy*, 2008, vol. 229, no. 2, p. 313 - 319.

[29] WANG, Z. J., DONG, J. F. Analysis of guided modes in asymmetric left-handed slab waveguides. *Progress in Electromagnetics Research*, 2006, vol. 62, p. 203 - 215.

[30] WANG, Z. H., XIAO, Z. Y., LUO, W. Y. Surface modes in left-handed material slab waveguides. *Journal of Optics A: Pure and Applied Optic*s, 2009, vol. 11, no. 1, 015101.

[31] HE, Y., CAO, Z., SHEN, Q. Guided optical modes in asymmetric left-handed waveguides. *Optics Communications*, 2005, vol. 245, no. 1-6, p. 125 - 135.

[32] WANG, Z. H., LI, S. P. Quasi-optics of the surface guided modes in a left-handed material slab waveguide. *Journal of the Optical Society of America B*, 2008, vol. 25, no. 6, p. 903 - 908.

[33] XIAO, Z. Y., WANG, Z. H. Dispersion characteristics of asymmetric double-negative material slab waveguides. *Journal of the Optical Society of America B*, 2006, vol. 23, no. 9, p. 1757 to 1760.

[34] TSAKMAKIDIS, K. L., HERMANN, C., KLAEDTKE, A., JAMOIS, C., HESS, O. Surface plasmon polaritons in generalized slab heterostructures with negative permittivity and permeability. *Physical Review B*, 2006, vol. 73, no. 8, 085104.

[35] PARK, K., LEE, B. J., FU, C., ZHANG, Z. M. Study of the surface and bulk polaritons with a negative index metamaterial. *Journal of the Optical Society of America B*, 2005, vol. 22, no. 5, p. 1016 to 1023.

[36] HE, Y., ZHANG, J., LI, C. Guided modes in a symmetric five-layer left-handed waveguide. *Journal of Optical Society of America B*, 2008, vol. 25, no. 12, p. 2081 - 2091.

[37] TAO, F., ZHANG, H. –F., YANG, X. –H, CAO, D. Surface plasmon polaritons of the metamaterial four-layered structures. *Journal of the Optical Society of America B*, 2009, vol. 26, no. 1, p. 50 - 59.

[38] CORY, H., ZACH, C. Wave propagation in metamaterial multi-layered structures. *Microwave and Optical Technology Letters*, 2004, vol. 40, no. 6, p. 460 - 465.

[39] D'AGUANNO, G., MATTIUCCI, N., SCALORA, M., BLOEMER, M. J. TE and TM guided modes in an air waveguide with negative-index-material cladding. *Physical Review E*, 2005, vol. 71, no. 4, 046603.

[40] JIANG, Y.–Y., SHEN, Z.–J. Guiding characteristics of an air waveguide with left-handed metamaterials cladding. *Journal of Nonlinear Optical Physics & Materials*, 2008, vol. 17, no. 4, p. 465 - 471.

[41] SATUBY, Y., KAMINSKY, N., ORENSTEIN, M. Nano-optical waveguide modes in gaps embedded in left-handed metamaterial. *Journal of the Optical Society of America B*, 2007, vol. 24, no. 10, p. A62 - A68.

[42] WANG, Z. H., XIAO, Z. Y., LI, S. P. Guided modes in slab waveguides with a left handed material cover or substrate. *Optics Communications*, 2008, vol. 281, no. 4, p. 607 - 613.

[43] HE, J., HE, S. Slow propagation of electromagnetic waves in a dielectric slab waveguide with a left-handed material substrate. *IEEE Microwave and Wireless Components Letters*, 2005, vol. 16, no. 2, p. 96 - 98.

[44] TASSIN, P., SAHYOUN, X., VERETENNICOFF, I. Miniaturization of photonic waveguides by the use of left-handed materials. *Applied Physics Letters*, 2008, vol. 92, no. 20, 203111.

[45] INAN, U. S. INAN, A. S. *Electromagnetic Waves*. Prentice Hall, 2000.

[46] RAETHER, H. *Surface Plasmons on Smooth and Rough Surfaces and on Gratings*. Berlin: Springer-Verlag, 1988.

[47] ALIEV, Yu. M., SCHLÜTER, H., SHIVAROVA, A. *Guided-Wave-Produced Plasmas*. Springer-Verlag, 2000.

[48] PRADE, B., VINET, J. Y., MYSYROWICZ, A. Guided optical waves in planar heterostructure with negative dielectric constant. *Physical Review B*, 1991, vol. 44, no. 24, p. 13556 - 13572.

[49] HOTTA, M., HANO, M., AWAI, I. Surface waves along a boundary of single negative material. *IEICE Transactions on Electronics*, 2005, vol. E88-C, no. 2, p. 275 - 278.

[50] ZHANG, H.–F., WANG, Q., SHEN, N.–H., LI, R., CHEN, J., DING, J., WANG, H.–T. Surface plasmon polaritons at interfaces associated with artificial composite materials. *Journal of Optical Society of America B*, 2005, vol. 22, no. 12, p. 2686 - 2696.

About Author

Ki Young KIM was born in Pohang, Korea in 1975. He received his B.S., M.S., and Ph.D. degrees in Electronics from Kyungpook National University (KNU), Daegu, Korea, in 1998, 2001, and 2005, respectively. He was a Brain Korea 21 Postdoctoral Research Fellow and Postdoctoral Research Associate at KNU from March 2005 to August 2006, then from September 2006 to August 2007 he was a Visiting Postdoctoral Fellow at Northwestern University, Evanston, Illinois, USA. Thereafter, he became a Senior Research Engineer for the Research and Development Division of the Hyundai Motor Company and Kia Motors Corporations, Hwaseong, Korea from October 2007 to October 2008. In October 2008, he joined the Department of Physics at National Cheng Kung University, Tainan, Taiwan, Republic of China as an Assistant Research Professor. His research interests include metamaterials, subwavelength plasmonics, nanophotonics, enhanced optical and microwave transmissions, and guided and leaky waves in electromagnetic waveguiding structures, among many others.